

# Development of an Optode for Detection of Trace Amounts of $\text{Hg}^{2+}$ in Different Real Samples Based on Immobilization of Novel Tetradentate Schiff Bases Bearing Two Thiol Groups in PVC Membrane

Ayman A. Abdel Aziz · Soha F. Mohammed ·  
Magdy M. El Gamel

Received: 28 December 2013 / Accepted: 3 February 2014  
© Springer Science+Business Media New York 2014

**Abstract** A very sensitive and reversible optical chemical sensor based on a novel tetradentate Schiff base namely N,N'-bis(2-aminothiophenol)benzene-1,2-dicarboxaldehyde (ATBD) immobilized within a plasticized PVC film for  $\text{Hg}^{2+}$  determination is described. At optimum conditions (i.e. pH 6.0), the proposed sensor displayed a linear response to  $\text{Hg}^{2+}$  over  $1.0 \times 10^{-10} - 1.0 \times 10^{-2} \text{ mol L}^{-1}$  with a limit of detection of  $7.23 \times 10^{-11} \text{ mol L}^{-1}$  ( $0.0145 \mu\text{g L}^{-1}$ ). Moreover, the results revealed that, under batch condition, the sensor is fully reversible within a response time  $\sim 35 \text{ s}$ . In addition to its high stability and reproducibility, the sensor showed good selectivity towards  $\text{Hg}^{2+}$  ion with respect to common metal cations. The sensor was successfully applied for determination of  $\text{Hg}^{2+}$  ion in some real samples, including hair, urine and well water samples. The results were in good correlation with the data obtained using cold vapor atomic absorption spectrometry.

**Keywords** NSSN Schiff base · PVC membrane · Fluorescent sensor ·  $\text{Hg}^{2+}$  ion

## Introduction

Development of sensitive chemosensors have been receiving much attention in recent years because of their potential applications in clinical biochemistry and environment. Metal-selective fluorescent chemosensors are served as useful tools for detection of metal ions due to their intrinsic sensitivity and selectivity [1, 2].

Chemical optical sensors (optodes) offer several advantages such as simple preparation procedure, relatively fast response, wide response range, reasonable selectivity and high sensitivity [3, 4]. The immobilization of various sensing reagents of optode membranes have been developed for many analytically relevant ions, especially heavy metal ions. Immobilization of dyes into or onto a solid support is a key issue for their application in optical sensing [5]. The reagent is normally physically entrapped by adsorption, electrostatic attraction or chemical bonding to the solid support. Generally, sol-gel glasses [6, 7] or polymer matrices [8, 9] are used for the preparation of the optodes. Poly(vinyl chloride) (PVC) has been used for the preparation of membrane optodes due to its relatively low cost, good mechanical properties and amenability to plasticization [10].

Mercury ion is one of the most prevalent toxic heavy metal ions causing environmental and health problems because of its wide distribution and severe immunotoxic, genotoxic, and neurotoxic effects [11–13].  $\text{Hg}^{2+}$  is a highly stable inorganic form of mercury, which, according EPA and WHO guidelines, must be in concentrations  $< 0.002 \text{ mg L}^{-1}$  in well water [14].

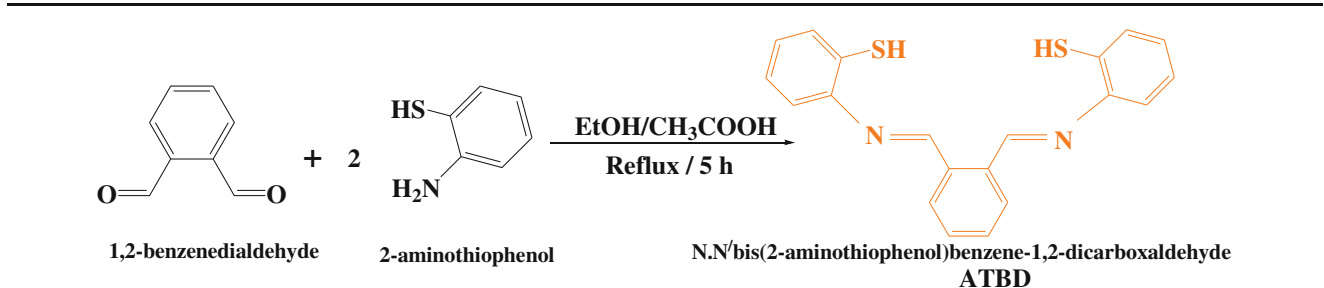
A. A. A. Aziz (✉)  
Department of Chemistry, Faculty of Science, Ain Shams University,  
11566 Cairo, Egypt  
e-mail: aymanaziz31@gmail.com

A. A. A. Aziz  
e-mail: aabelaziz@ut.edu.sa

A. A. A. Aziz  
Department of Chemistry, Faculty of Science, University of Tabuk,  
Tabuk 71421, Saudi Arabia

S. F. Mohammed · M. M. El Gamel  
Department of Chemistry, Faculty of Science, Zagazig University,  
44519 Zagazig, Egypt

M. M. El Gamel  
Department of Chemistry, College of Sciences and Humanities,  
Shaqra University, Aldawadmi 11911, Saudi Arabia



**Scheme 1** Synthetic route of ATBD

Many current techniques for mercury screenings were assigned such as atomic absorption spectrometry [15–18], inductively coupled plasma-mass spectroscopy [19–21], X-ray fluorescence spectrometry [22, 23], neutron activation analysis [24, 25], cold vapor atomic absorption spectrometry [26], electrothermal atomic absorption spectrometry [27–29], anodic stripping voltammetry [30–33], high-performance liquid chromatography [34–36], atomic fluorescence spectrometry [37], potentiometric ion-selective electrodes [38–40] and spectrophotometry [41–50].

Most of these methods suffer from some problems such as poor reproducibility, limited sample adaptability, high cost, well-controlled experimental conditions, multi-step sample pre-treatments, some inherent interference, time consuming procedures and too expensive involving the use of sophisticated instrumentation, the wide utilization of these methods is largely limited. So, for simplicity, convenience, no necessity of the reference solution, low cost, and fieldwork applicability the easily prepared optical sensors are highly demanding.

Recently, some selective fluorescent chemosensors for  $\text{Hg}^{2+}$  based on fluorescence enhancement or fluorescence quenching has been reported [51–67]. However, most of them have disadvantage in practical use, such as low water solubility, interference from other metal ions, strict reaction condition or complicated synthetic route. Therefore, development of simple fluorescent chemosensor that can selectively sense  $\text{Hg}^{2+}$  in aqueous media is significant. In construction of optical sensors Schiff's base ligands have been frequently used as

ionophores in construction of membrane sensors because of their ability to form stable complexes with transition metal ions. They produce remarkable selectivity, sensitivity and stability for a specific ion [68–71].

Keeping these facts in mind, in this work, we develop an optode for sensitive and selective determination of  $\text{Hg}^{2+}$ . This optode is prepared by immobilizing a novel tetradentate Schiff base bearing two thiol groups as the sensing reagent in PVC membrane according to a simple method. The membrane sensitivity, selectivity, reproducibility, short-term stability, lifetime and regeneration under optimum conditions were fully studied. Moreover, the response mechanism and binding mode were investigated by  $^1\text{H}$  NMR and TOF-MS. Finally, the novel sensor was applied for determination of  $\text{Hg}^{2+}$  ion in some different real samples, including hair, urine and well water samples.

## Experimental

## Instruments

All fluorescence measurements were carried out on a Jenway 6270 Fluorimeter. The excitation source was a Pulsed Xenon Lamp. The UV–Vis spectra were recorded on a Shimadzu UV 1800 Spectrophotometer. pH measurements were performed by Jenway pH meter model 3510 equipped with Glass bodied combination pH electrode (924005) and calibrated with Meck pH standards of pH 4.00, 7.00, and 10.00. All of the experiments were carried out at room temperature  $25 \pm 1$  °C. FT-IR spectrum of the ionophore was obtained in KBr discs on a Unicam-Mattson 1000 FT-IR.  $^1\text{H}$  NMR spectra were performed on a 300 MHz NMR spectrometer in  $\text{DMSO}-d_6$  solvent and TMS was used as an internal reference. Mass spectra (TOF-MS) were recorded on Waters (USA) KC-455 model with  $\text{ES}^+$  mode in DMSO.

## Materials and Reagents

2-aminothiophenol, benzene-1,2-dicarboxaldehyde (o-phthaldialdehyde) and the lipophilic anionic additive reagent potassium tetrakis-(4-chlorophenyl) borate (KTpClPB) were supplied from Aldrich. The polymer membrane components, polyvinyl

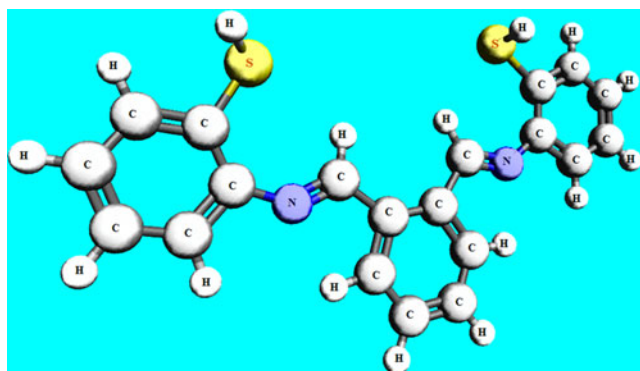
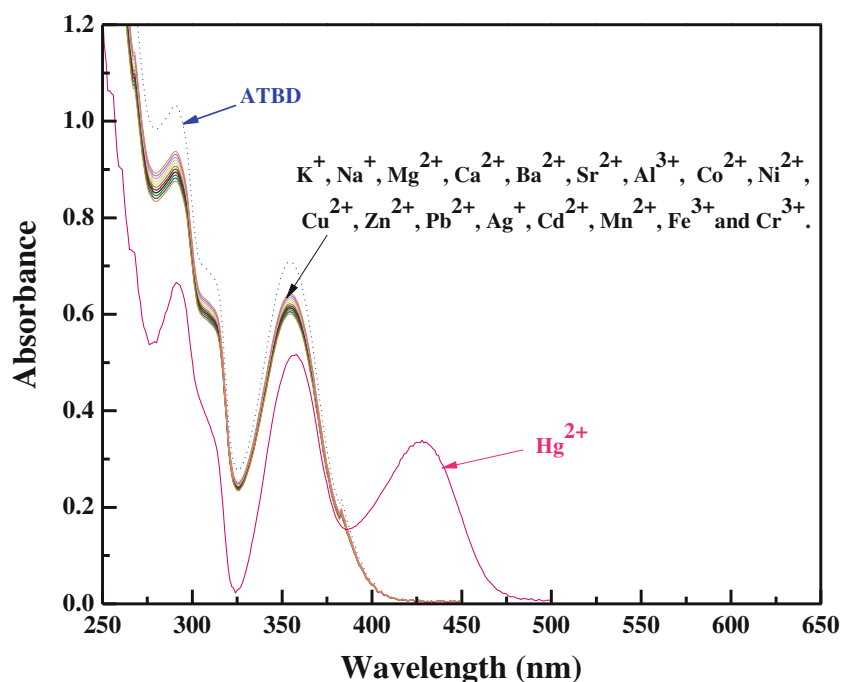


**Fig. 1** Optimal structure of the chemosensor (ATBD)

**Fig. 2** UV–Vis absorption spectra of ATBD (2.0  $\mu\text{M}$ ) with 1 equivalent metal ions ( $\text{K}^+$ ,  $\text{Na}^+$ ,  $\text{Mg}^{2+}$ ,  $\text{Ca}^{2+}$ ,  $\text{Ba}^{2+}$ ,  $\text{Sr}^{2+}$ ,  $\text{Al}^{3+}$ ,  $\text{Co}^{2+}$ ,  $\text{Ni}^{2+}$ ,  $\text{Cu}^{2+}$ ,  $\text{Zn}^{2+}$ ,  $\text{Pb}^{2+}$ ,  $\text{Ag}^+$ ,  $\text{Cd}^{2+}$ ,  $\text{Mn}^{2+}$ ,  $\text{Fe}^{3+}$ ,  $\text{Cr}^{3+}$  and  $\text{Hg}^{2+}$ )



chloride (PVC) (high molecular weight) and the plasticizers, bis-(2-ethylhexyl) phthalate (DOP), bis(2-ethylhexyl)sebacate (DOS), bis-(2-ethylhexyl) adipate (DAO) and 2-nitrophenyl octyl ether (NPOE) were obtained from Fluka. Absolute ethanol (EtOH), tetrahydrofuran (THF), and dichloromethane (DCM) were purchased from Merck. All solvents were of analytical grade and they were used as received. A stock solution of  $1.0 \times 10^{-2}$  M was prepared by dissolving 0.3606 g of  $\text{Hg}(\text{NO}_3)_2 \cdot 2\text{H}_2\text{O}$  in exactly 100 ml of deionized water and standardized with the EDTA solution [72]. The stock solution was serially diluted to achieve the desired concentrations.

#### Synthesis of N,N'-bis(2-aminothiophenol) benzene-1,2-dicarboxaldehyde (ATBD)

An ethanolic solution of 2-amiothiophenol (10 mmol) was mixed with an ethanolic solution of o-phaldehyde (5 mmol), 2 drops of acetic acid and magnetically stirred in a round bottom flask. The reaction mixture was then refluxed for ~5 h at 60 °C in water bath and kept overnight. The resulting solution was then poured into crushed ice water. The precipitate formed was filtered and recrystallized from hot methanol and dried in a desiccator over anhydrous  $\text{CaCl}_2$  under vacuum to get chromatographically (TLC) pure compound. Synthetic route of ATBD is shown in Scheme 1.

Characteristics of ATBD were as follows ( $\text{C}_{20}\text{H}_{16}\text{N}_2\text{S}_2$ ): M.Wt: 348.494 Yield: 87 %. Color: Orange. Elemental analysis Calc. (%): C, 68.93; H, 4.62; N, 8.03 Found: C, 68.40; H, 4.39; N, 8.00. IR (KBr pellet.  $\text{cm}^{-1}$ ): 2543 ( $\nu_{\text{SH}}$ ); 1612 ( $\nu_{\text{C=N}}$ ); 798 ( $\nu_{\text{C-S}}$ ).  $^1\text{H}$  NMR (DMSO- $d_6$ , 300 MHz):  $\delta$  3.64 (s, 2H; SH); 8.23 (s, 2H; HC=N); 6.74–7.57 (m, 14H;

aromatic). TOF-MS ( $m/z$ ): 348 ( $\text{M}^+$ ). The optimal structure of the chemosensor (ATBD) is shown in Fig. 1 by using Avogadro program Version 1.0.1.

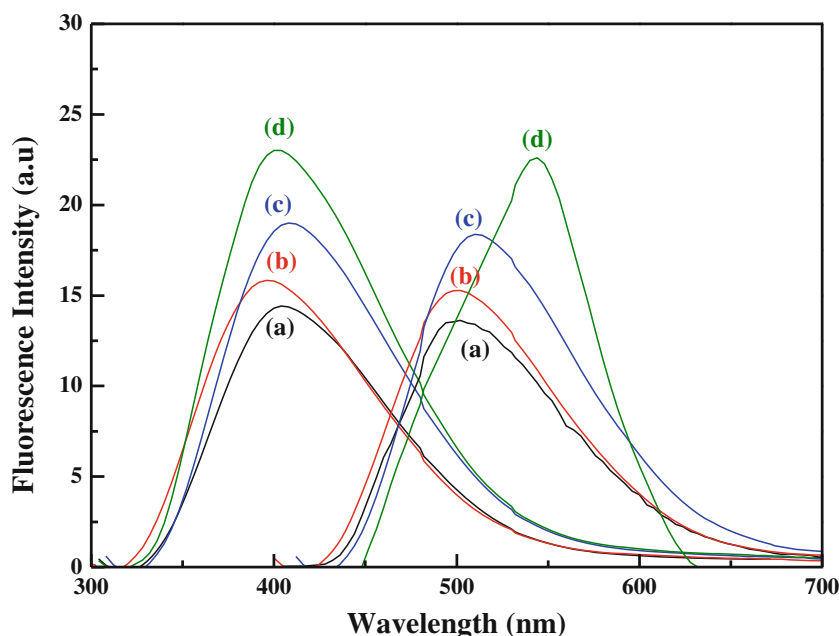
#### Preparation of the Optode Membrane

Membrane solutions were prepared by dissolving 30 mg of PVC, 65 mg of plasticizer (DOS), 2.0 mg of KTpClPB and 3.0 mg ATBD in 2.0 ml THF. The solution was stirred with a magnetic stirrer to obtain a homogeneous mixture. Glass slides for bulk measurements were cut from microscope slides into 12 mm  $\times$  16 mm dimensions to fit precisely into its diagonal width of standard quartz cell. To improve the adhesion of the membrane, the glass slides were cleaned with THF, sulfuric acid and sodium hydroxide solutions, respectively, then thoroughly rinsed with deionized water and finally dried in an oven



**Fig. 3** The color change of the sensor upon complexation with  $\text{Hg}^{2+}$  ions (1 ATBD; 2 ATBD +  $\text{Hg}^{2+}$ )

**Fig. 4** Emission and excitation spectra of ATBD in (a) DCM, (b) THF, (c) EtOH and (d) PVC



at 110 °C. Membranes were cast by placing 35  $\mu\text{l}$  of the membrane solution onto the glass slide of  $\sim 10\ \mu\text{m}$  thickness and spread evenly using a capillary glass tube [73, 74]. The thickness of the films was in the order of 3–4  $\mu\text{m}$  (as evaluated from the volume employed for spreading). After 2 min. the coated slides were transferred to a Petri dish with a filter paper cover and then stored away from light for 12 h before use. Blank (reference) membranes were prepared in a similar way excluding ATBD from the membrane solution. Absorption and fluorescence emission spectra of PVC membranes were recorded in quartz cells which were filled with sample solution. The polymer films were placed in diagonal position in the quartz cell. All of the experiments were operated at room temperature ( $25 \pm 1\ ^\circ\text{C}$ ). The membranes were not conditioned before use.

#### Measurement Procedure

The membranes were diagonally placed inside the sample cuvette of the instrument containing 2 ml buffer solution of pH 6.0 and a blank membrane (without ionophore) was put in the reference cuvette containing the buffer solution. The fluorescence intensity at an excitation wavelength of 403 nm was measured at 544 nm. The sample was then titrated with a standard  $\text{Hg}^{2+}$  ion solution using a pre-calibrated micropipette and the fluorescence intensity of the system was measured after  $\sim 35\ \text{s}$  (required to reach equilibrium).

#### Preparation of Real Samples

##### Hair Samples

Scalp hair samples as a suitable specimen for monitoring human exposure to mercury, were used in this study. The hair

sample was first soaked in deionized water for 10 min. This was followed by soaking in 1 % triton X-100 solution for 20 min [75]. The hair sample was then rinsed five times with deionized water and air-dried. 0.250 g of dried hair sample was digested with 5.0 ml 0.1 M  $\text{HNO}_3$  for 2 h at  $\sim 120\ ^\circ\text{C}$ . Finally 3.0 ml of  $\text{H}_2\text{O}_2$  was added to the sample and digested. The residue was diluted with deionized water to 50.0 ml volumetric flask.

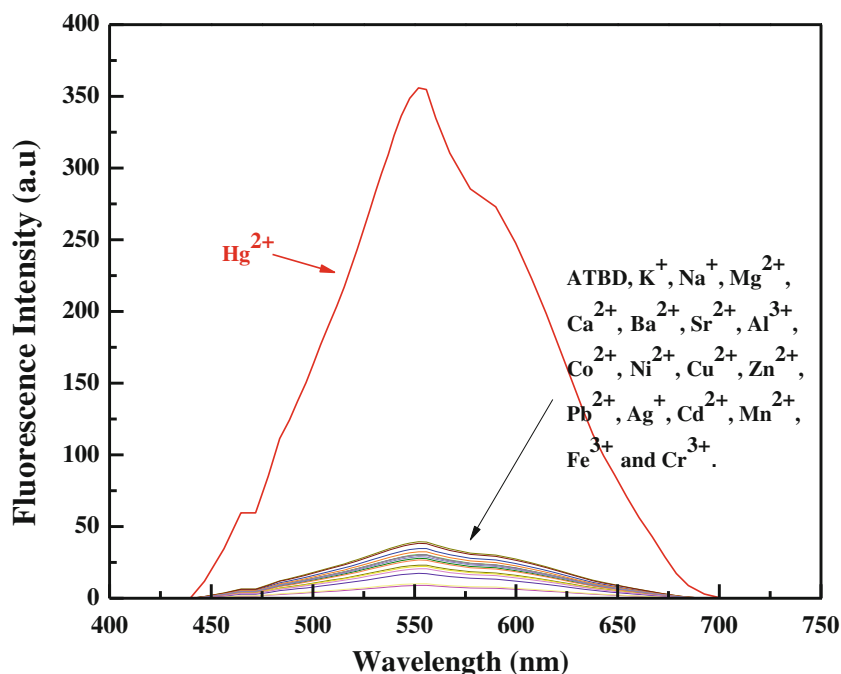
##### Urine Samples

Most mercury present in the urine is in the form of inorganic mercury. The mercury concentration in the urine increases in relation to the level of inorganic mercury accumulated in the kidneys [76]. Accordingly, the total mercury value in the urine is an important biomarker for evaluating inorganic mercury/mercury vapor exposure. Dental clinics are known to be one of the largest users of inorganic and metallic mercury [77]. Mercury, which vaporizes at room temperature and easily enters the environment, is used in the preparation of amalgam alloy

**Table 1** Emission and excitation spectral data of ATBD in various solvents and PVC membrane

Solvent	Polarity index (P)	Wavelength (nm)		Stokes shift	Refractive index
		$\lambda_{\text{ex}}$	$\lambda_{\text{em}}$	$\Delta\lambda_{\text{ST}}$ (nm)	$\eta$
DCM	3.1	406	502	96	1.42
THF	4	400	498	98	1.40
EtOH	5.2	408	510	102	1.36
PVC	—	403	544	141	1.52

**Fig. 5** Emission spectra of ATBD sensing membrane after exposure to 1.0  $\mu\text{M}$  different metal ions ( $\text{K}^+$ ,  $\text{Na}^+$ ,  $\text{Mg}^{2+}$ ,  $\text{Ca}^{2+}$ ,  $\text{Ba}^{2+}$ ,  $\text{Sr}^{2+}$ ,  $\text{Al}^{3+}$ ,  $\text{Co}^{2+}$ ,  $\text{Ni}^{2+}$ ,  $\text{Cu}^{2+}$ ,  $\text{Zn}^{2+}$ ,  $\text{Pb}^{2+}$ ,  $\text{Ag}^+$ ,  $\text{Cd}^{2+}$ ,  $\text{Mn}^{2+}$ ,  $\text{Fe}^{3+}$ ,  $\text{Cr}^{3+}$ ,  $\text{Al}^{3+}$  and  $\text{Hg}^{2+}$ )



that consists chiefly of silver mixed with mercury and variable amounts of other metals and is used as a dental filling. It is well documented that dentists who work with amalgam are chronically exposed to mercury vapors, which can accumulate in their bodies to much more higher levels than for most non-occupationally exposed individuals. 24-h urine samples were obtained from dentists who had several months of steady exposure, at the end of a working week in 2.5 l polypropylene sampling vessels followed by the addition of concentrated  $\text{HNO}_3$  to yield a final acid concentration of 1–3 % v/v and the samples were stored at  $-20^\circ\text{C}$  prior to analysis.

#### Preparation of Well Water Samples

Before the analysis, water samples were filtered through a Whatman No. 41 filter paper. The organic content of the water

samples were oxidized in the presence of 1 %  $\text{H}_2\text{O}_2$  followed by addition of concentrated nitric acid, then the pH of water samples was adjusted to 6.0.

## Results and Discussion

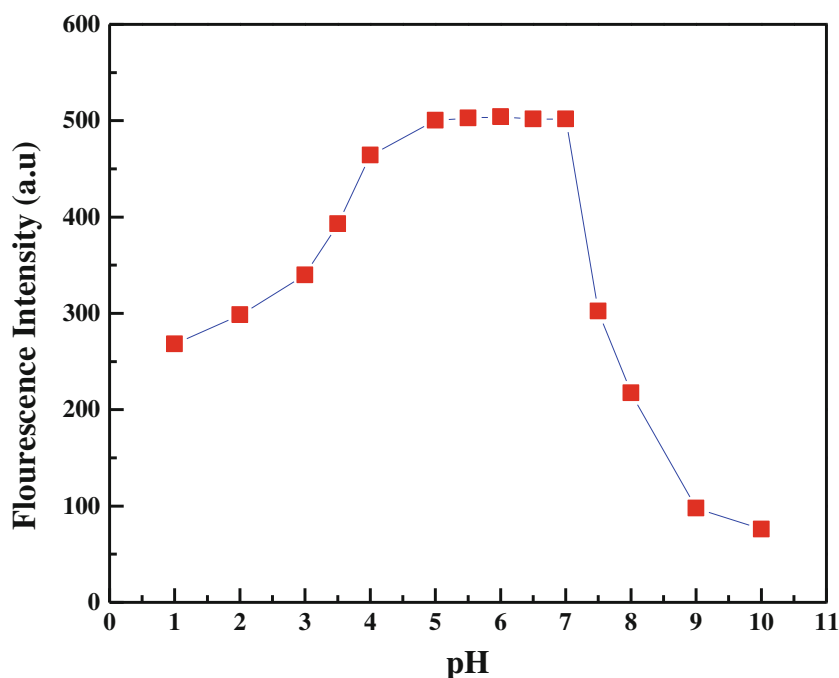
### UV–Vis Spectral Responses of ATBD

It has been anticipated that, due to the presence of various donor sites in the form of N and S atoms, ATBD would behave as a potential ligand for complexation reaction with metal ions. To explore the properties of ATBD as an optically sensing material, various metal ions were tested in a preliminary experiment. The binding affinity of ATBD was monitored through absorption spectra of ATBD ( $2.0\ \mu\text{M}$ ) in

**Table 2** The effect of membrane ingredients on the response behavior of optodes ( $n=5$ )

Optode No.	PVC (mg)	Plasticizer (mg)	KTpClPB (mg)	ATBD (mg)	Working concentration range ( $\text{mol L}^{-1}$ )	Response time (sec)
1	30	NPOE (67)	0	3	$6.4 \times 10^{-7}$ to $2.0 \times 10^{-5}$	120
2	30	DOA (67)	0	3	$2.6 \times 10^{-6}$ to $1.0 \times 10^{-5}$	150
3	30	DOP (67)	0	3	$5.0 \times 10^{-7}$ to $3.0 \times 10^{-4}$	200
4	30	DOS (67)	0	3	$1.0 \times 10^{-8}$ to $3.0 \times 10^{-4}$	80
6	30	DOS (66)	1	3	$1.3 \times 10^{-9}$ to $2.0 \times 10^{-3}$	60
7	30	DOS (65)	2	3	$1.0 \times 10^{-10}$ to $1.0 \times 10^{-2}$	35
8	30	DOS (64)	3	3	$6.4 \times 10^{-7}$ to $4.0 \times 10^{-5}$	80
9	30	DOS(64)	4	2	$8.0 \times 10^{-7}$ to $3.0 \times 10^{-3}$	100
10	30	DOS (64)	5	1	$2.0 \times 10^{-6}$ to $3.0 \times 10^{-3}$	130

**Fig. 6** Effect of pH on the response of the ATBD optode in the presence of 1.0  $\mu\text{M}$   $\text{Hg}^{2+}$  at 544 nm ( $\lambda_{\text{ex}}$  403 nm)



absence and presence of 1 equivalent tested metal ions of  $\text{K}^+$ ,  $\text{Na}^+$ ,  $\text{Mg}^{2+}$ ,  $\text{Ca}^{2+}$ ,  $\text{Ba}^{2+}$ ,  $\text{Sr}^{2+}$ ,  $\text{Al}^{3+}$ ,  $\text{Co}^{2+}$ ,  $\text{Ni}^{2+}$ ,  $\text{Cu}^{2+}$ ,  $\text{Zn}^{2+}$ ,  $\text{Pb}^{2+}$ ,  $\text{Ag}^+$ ,  $\text{Cd}^{2+}$ ,  $\text{Mn}^{2+}$ ,  $\text{Fe}^{3+}$ ,  $\text{Cr}^{3+}$  and  $\text{Hg}^{2+}$  (Fig. 2). As shown in Fig. 2, ATBD shows two absorption bands, the first at 293 which can be assigned to  $\pi$ - $\pi^*$  transitions from the benzene ring and the double bond of the azomethine group and the second at 356 nm due to  $n$ - $\pi^*$  transition of non-bonding electrons present on the nitrogen of the azomethine group. Upon addition of addition of  $\text{Hg}^{2+}$ , the color of ATBD solution concomitantly, changes from yellow-orange to a pink (Fig. 3), inducing a bathochromic shift of ATBD bands and a new band was originated at 428 nm, which may assigned to charge transfer. In contrast, addition of other metal ions showed insignificant changes. The results demonstrated that ATBD is characteristic of high selectivity toward  $\text{Hg}^{2+}$  over other competitive metal ions.

#### Fluorescence Spectral Responses of ATBD

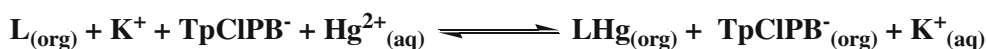
In order to perform the fluorescence characterization of the ATBD, the emission and excitation spectra of ATBD were recorded in solvents of different polarities and PVC matrix. The gathered excitation-emission spectra are shown in Fig. 4. The Stokes shift values,  $\Delta\lambda_{\text{ST}}$  (the difference between excitation and emission maxima) were extracted from spectral data which are given in Table 1. Since larger Stokes shifts are obtained in polar solvents [78], the highest Stokes shift for

the ATBD was observed in EtOH. Moreover, ATBD exhibited higher fluorescence intensity in PVC matrix compared to that in the solvents. The immobilization of ATBD molecules in solid matrix may reduce intramolecular motions and rearrangements, thus leading to enhanced fluorescence capability.

In order to explore the selective sensing of ATBD towards  $\text{Hg}^{2+}$ , fluorescence spectra of ATBD immobilized on PVC membrane were measured in EtOH with respective metal ions including  $\text{K}^+$ ,  $\text{Na}^+$ ,  $\text{Mg}^{2+}$ ,  $\text{Ca}^{2+}$ ,  $\text{Ba}^{2+}$ ,  $\text{Sr}^{2+}$ ,  $\text{Al}^{3+}$ ,  $\text{Co}^{2+}$ ,  $\text{Ni}^{2+}$ ,  $\text{Cu}^{2+}$ ,  $\text{Zn}^{2+}$ ,  $\text{Pb}^{2+}$ ,  $\text{Ag}^+$ ,  $\text{Cd}^{2+}$ ,  $\text{Mn}^{2+}$ ,  $\text{Fe}^{3+}$ ,  $\text{Cr}^{3+}$  and  $\text{Hg}^{2+}$  (Fig. 5). As in shown in Fig. 5, ATBD exhibit weak fluorescence emission when excited at 403 nm and when  $\text{Hg}^{2+}$  (1.0  $\mu\text{M}$ ) was added, a prominent fluorescent enhancement was observed at 544 nm and it was found that the other studied ions didn't induce any apparent fluorescent enhancement.

#### Optimization of Composition of the Membrane Components

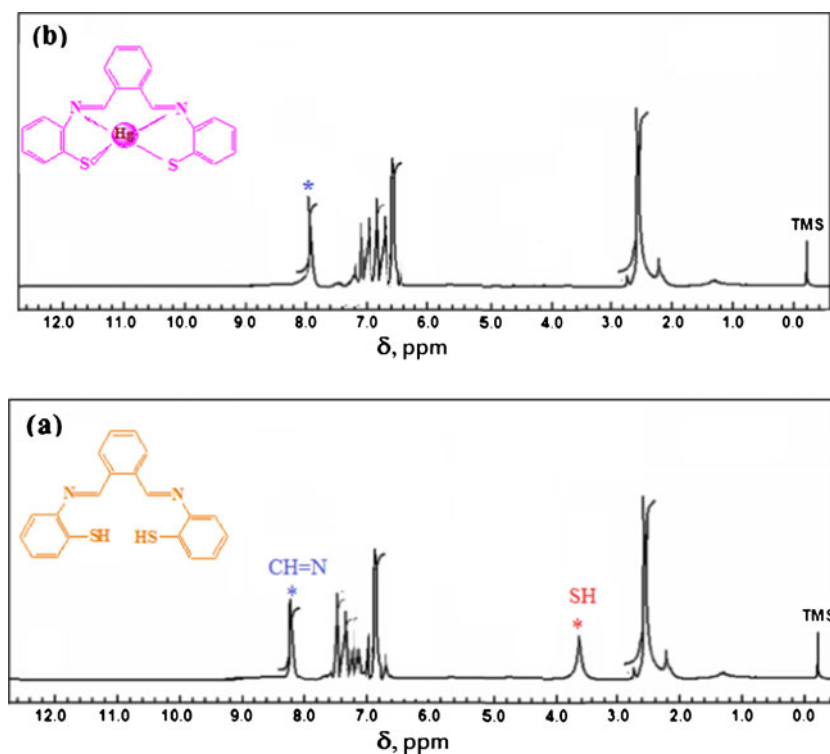
The response characteristics and working concentration range of optical membrane sensors are known to be largely affected by changes in the membrane composition [9, 79]. A comparative study on the effect of different plasticizers and matrix materials on the performance of sensor has been made. Several optode membranes were prepared using different plasticizers such as DOP, DOS, DAO, NPOE and the fluorescence measurements were made for different concentrations of



**Scheme 2** Response mechanism of immobilized ATBD on PVC membrane towards  $\text{Hg}^{2+}$



**Fig. 7**  $^1\text{H}$  NMR spectra of sensor ATBD (1.0  $\mu\text{M}$ ) with  $\text{Hg}^{2+}$  in  $d_6$ -DMSO: (a) ATBD and (b) ATBD +  $\text{Hg}^{2+}$  (1.0 eq.)



$\text{Hg}^{2+}$ . The results are shown in Table 2. The widest working concentration range was obtained with DOS; therefore, this plasticizer was used for further studies. Lipophilic borate salts are frequently used as anionic additives in potentiometric and optical cation-selective sensors based on solvent polymeric membranes [80]. The amount of anionic sites in the membranes has effects on the linear range and selectivity of optodes [8]. The composition of the optode membrane with respect to KTpCIPB was optimized by preparing several membranes with different amounts of KTpCIPB. The response behavior of these optode membranes are shown in Table 2. From the results it can be seen that the response concentration range of the optode membrane becomes wider with shorter response time as the amount of KTpCIPB in the optode membrane increases from 1 % to 2 %, which might be attributed to the increasing of hydrophilicity upon addition of KTpCIPB. However, the response concentration range of the optode membrane becomes narrower when the content of KTpCIPB is larger than 2 %. Therefore, 2 % KTpCIPB provided the best response for  $\text{Hg}^{2+}$  and was chosen for further studies.

The data given in Table 2 give an indication of the pronounced influence of the amount of the ionophore on the working range of the proposed optical sensor. As it can be seen, an increase in the amount of ATBD from 1 % to 3 % resulted in an improved lower limit of the working range, emphasizing the expected increase in the sensitivity of the optical sensor in the presence of increased amount of the ionophore in the membrane phase.

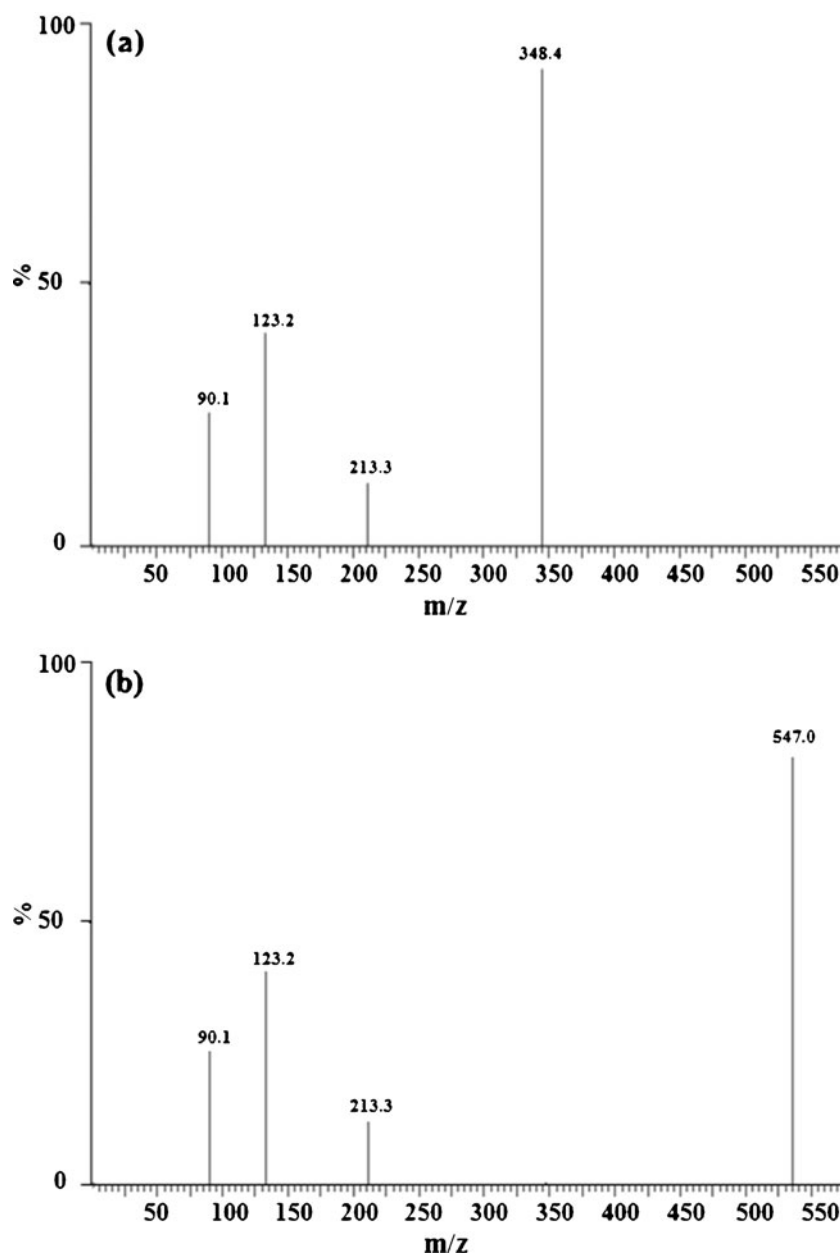
#### Effects of pH

The effect of the pH of the solution, in which the sensor is applied is a critical factor that must be considered definitely. To study the effect of pH on the optode response to  $\text{Hg}^{2+}$ , the fluorescence intensity versus pH plot was obtained by changing the solution pH with different buffer solutions and fixing the  $\text{Hg}^{2+}$  concentration at 1.0  $\mu\text{M}$  (Fig. 6). The pH of solution was adjusted by buffers of  $\text{CH}_3\text{COOH}/\text{NaCH}_3\text{COONa}$  Tris-HCl buffer and  $\text{NH}_4\text{Cl}/\text{NH}_3$ . As it is seen, the response of the sensor increased with increasing pH value of solution and reached a plateau between pH 5.0 and 7.0. At  $\text{pH} < 5.0$  the fluorescence response of the sensor membrane decreased with decreasing pH value due to proton binding by imine nitrogen [81] and on the other hand, the diminished fluorescence response at  $\text{pH} > 7.0$  could be attributed to the formation of  $\text{Hg}^{2+}$  ion hydroxides [82], as well as a possible slight swelling of the polymeric film under alkaline conditions. Hence, in the subsequent experiments, the pH values of all solutions were adjusted to 6.0 for further studies.

#### Response Mechanism, Binding Mode and Measuring Range

Among the various detection systems used in mercury optodes, those based on sulfur-containing ligands. Generally, these systems have shown better selectivity and sensitivity [82].  $\text{Hg}^{2+}$  displays great affinity for soft coordination centers like sulfur [83, 84], therefore, ligand ATBD with sulfur-containing sites was investigated as an active ionophore for

**Fig. 8** TOF-MS spectra of sensor ATBD (1.0  $\mu\text{M}$ ) with  $\text{Hg}^{2+}$  in  $d_6$ -DMSO: (a) ATBD and (b) ATBD +  $\text{Hg}^{2+}$  (1.0 eq.)



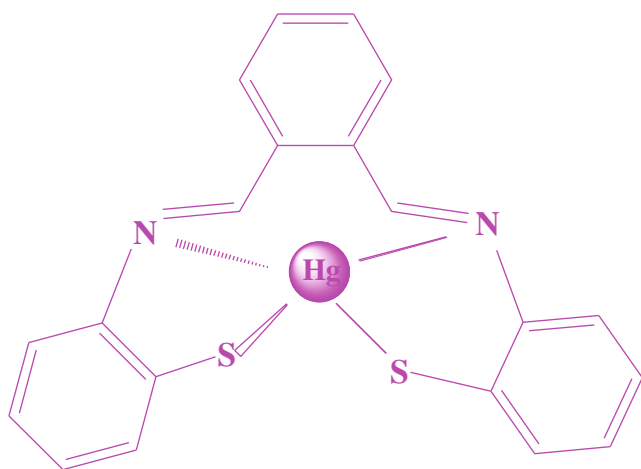
highly selective and sensitive determination of mercury ion.  $\text{Hg}^{2+}$  bonding takes place with NSSN donor sites of the azomethine  $-\text{N}$  and thiophenolate  $-\text{S}$  [85]. When ATBD ( $\text{LH}_2$ ) was doped in plasticized PVC together with the anionic additive  $\text{KTPCIPB}$  at pH 6.0, the system becomes a selective  $\text{Hg}^{2+}$  sensor. Furthermore, the fluorescence intensities of the optode membrane gradually increased with increasing  $\text{Hg}^{2+}$  concentrations, which constitutes the basis for the determination of  $\text{Hg}^{2+}$  with the proposed sensor proposed in this work. The lipophilic anionic sites, i.e.  $\text{TPCIPB}^-$  provide the optode membrane with the necessary ion-exchange properties because the fluoroionophore acts as a neutral ligand, and hence can't function as an ion exchanger. The overall equilibrium

between the aqueous sample solution (aq) and the organic membrane phase (org) is represented in Scheme 2.

The enhancement of the fluorescence of  $\text{Hg}^{2+}$  complex compared to the parent ligand may be due to CHEF (chelation enhancement of fluorescence emission) [86]. Factors like a simple binding of the ligand to the metal ions [87], an increase in rigidity in structure [88], a restriction in the photo induced electron transfer (PFT) [89, 90] etc. are assigned to the appearance and enhancement of the photoluminescence (PL). In the present case, the first two factors seem to be responsible for the enhancement PL.

For elucidation the binding mode, the  $^1\text{H}$  NMR-titration experiments were carried out. As shown in Fig. 7, the  $^1\text{H}$





**Scheme 3** Plausible interaction mode of ATBD/ $\text{Hg}^{2+}$

NMR spectrum of ATBD showed a singlet signal at  $\delta$  3.64 ppm which was attributed to thiol -SH protons. Upon addition of  $\text{Hg}^{2+}$ , the SH signal disappeared, which suggested that a  $\text{Hg}^{2+}$  bound to the two sulphur atoms of the ATBD backbone via deprotonation of SH groups. The singlet signal at  $\delta$  8.23 ppm in the parent ATBD which was attributed to the azomethine (-CH=N-) protons displayed an upper field shift ( $\delta$  7.94) upon the addition of  $\text{Hg}^{2+}$  which originated from the coordination of the azomethine nitrogen to  $\text{Hg}^{2+}$ . Moreover, the binding mode of ATBD ( $\text{LH}_2$ ) with  $\text{Hg}^{2+}$  was also examined by TOF-MS spectra (Fig. 8). The positive-ion mass spectrum of ATBD upon addition of  $\text{Hg}^{2+}$  (1 equiv) exhibited one intense peak at  $m/z=547$ , corresponding to the ion  $[\text{HgL}]$ , corroborating the 1:1 binding stoichiometry of  $\text{LH}_2$  (ATBD)

with  $\text{Hg}^{2+}$ . Taken together, the above results indicated a plausible interaction mode of ATBD/ $\text{Hg}^{2+}$  as proposed in Scheme 3, in which  $\text{Hg}^{2+}$  ion was coordinated with two “N” and two “S” atoms of ATBD.

Figure 9 shows the fluorescence emission spectra of the sensing membrane exposed to the solutions containing different concentrations of  $\text{Hg}^{2+}$  ( $\lambda_{\text{ex}}$  403 nm). The linearity was determined by plotting the fluorescence enhancement value  $\Delta F$  ( $\Delta F = F - F_0$ , where  $F_0$  and  $F$  were the fluorescence emission intensities before and after addition of  $\text{Hg}^{2+}$ ) against the negative logarithm of  $\text{Hg}^{2+}$  concentration, obtaining a linear equation of  $\Delta F = 995.99 + 84.689 \log [\text{Hg}^{2+}]$  ( $R=0.9948$ ) in the concentration range of  $1.0 \times 10^{-10}$  to  $1.0 \times 10^{-2}$  mol  $\text{L}^{-1}$  (Fig. 10). The limit of detection (LOD) based on  $3\sigma$  of the blank was  $7.23 \times 10^{-11}$ .

#### Response Time, Reproducibility, Short-Term Stability, Lifetime and Regeneration

The dynamic response time, is an important analytical feature of any optode. The response time was tested by recording the fluorescence intensity change from a buffered solution at pH=6 to a buffered  $\text{Hg}^{2+}$  solution over a wide concentration range ( $1.0 \times 10^{-10}$  to  $1.0 \times 10^{-2}$  mol  $\text{L}^{-1}$ ). The resulting intensity–time curve (Fig. 11) revealed that, the fluorescence intensity of the corresponding signal reached its equilibrium response in a relatively short time of less than 35 s. It was obvious that the response time is lower in concentrated solutions than dilute solutions.

The repeatability and reproducibility of optical sensors are two of their important characteristic features both of which

**Fig. 9** Emission spectra of ATBD sensing membrane after exposure to different  $\text{Hg}^{2+}$  concentrations ( $1.0 \times 10^{-10}$ – $1.0 \times 10^{-2}$  mol  $\text{L}^{-1}$ ) at pH=6.0. Dashed curve represent blank solution and arrows show the changes in fluorescence intensity with respect to an increase of  $\text{Hg}^{2+}$  concentration ( $\lambda_{\text{ex}}$  403 nm and  $\lambda_{\text{em}}$  544 nm)

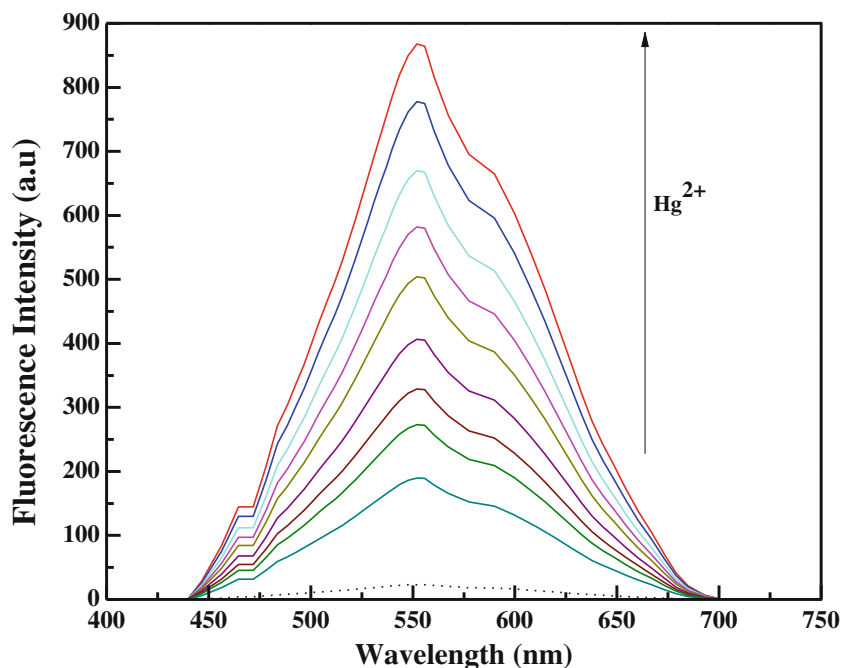
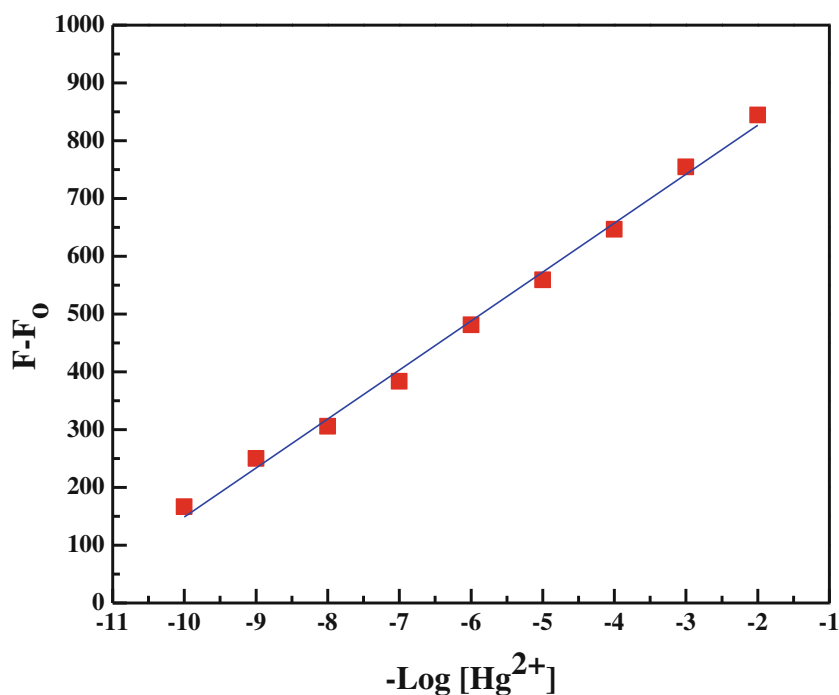


**Fig. 10** Calibration plot of the sensor in the concentration range of  $1.0 \times 10^{-10}$ – $1.0 \times 10^{-2}$  mol L $^{-1}$  at pH=6.0 in EtOH ( $\lambda_{\text{ex}}$ =403 nm)



were studied in this work. The reproducibility was examined by preparing 8 different membranes from the same mixture and measuring the fluorescence of each membrane at 544 nm using 1.0  $\mu$ M Hg $^{2+}$  (three repeated determinations) in the buffer solutions at pH 6.0. The resulting coefficient of variation was found to be  $\pm 1.7$  %. The short-term stability of the optical sensor was studied by measuring its fluorescence intensity in contact with 1.0  $\mu$ M Hg $^{2+}$  at pH 6.0 over a period of 10 h. From the fluorescence measurements, after every 60 min ( $n=10$ ), it

was found that the response was almost complete with only 2.5 % change in the fluorescence after 10 h monitoring. In addition, it was found that the membrane sensor could be stored in wet conditions without any measurable changes in its fluorescence for at least 15 weeks, which implies that the ionophore is quite stable in the membrane. Thus, the membrane sensor was immersed in the buffer solution of pH 6.0 when not in use.

The reversibility of the optode was checked by washing the used optodes with 0.2 mol L $^{-1}$  thiocyanate and/or iodate

**Fig. 11** Dynamic response of the proposed fluorescence membrane sensor for step change in concentration of Hg $^{2+}$  ion at pH=6.0: (a)  $1.0 \times 10^{-2}$ , (b)  $1.0 \times 10^{-3}$ , (c)  $1.0 \times 10^{-4}$ , (d)  $1.0 \times 10^{-5}$ , (e)  $1.0 \times 10^{-6}$ , (f)  $1.0 \times 10^{-7}$ , (g)  $1.0 \times 10^{-8}$ , (h)  $1.0 \times 10^{-9}$ , (i)  $1.0 \times 10^{-10}$

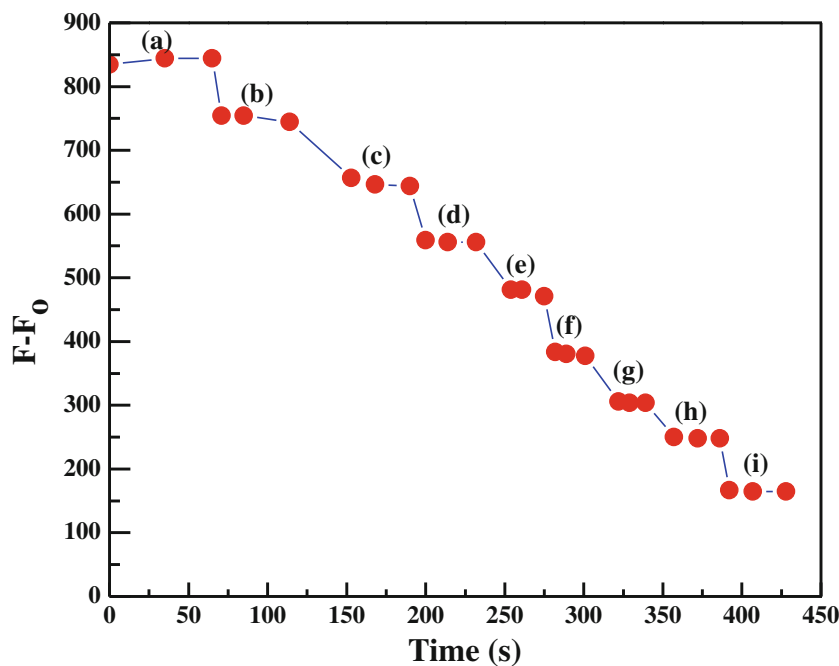
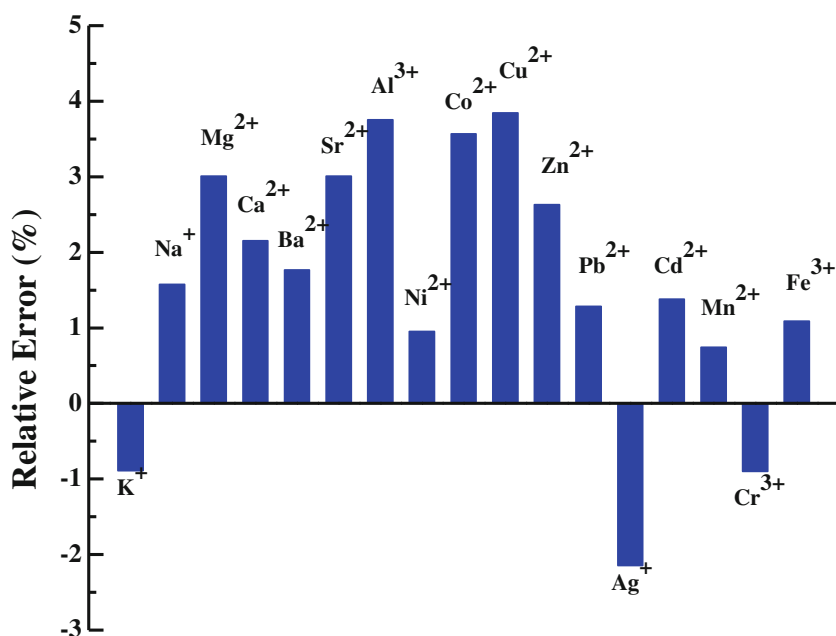


**Fig. 12** Interferences of different metal ions ( $1.0 \times 10^{-2} \text{ mol L}^{-1}$ ) onto the fluorescence determination of  $\text{Hg}^{2+}$  ion ( $1.0 \times 10^{-10} \text{ mol L}^{-1}$ ) using the proposed membrane sensor at pH 6.0



solutions. The results showed that the optodes were not regenerated to use one more time for  $\text{Hg}^{2+}$  determination. In addition, HCl and/or  $\text{HNO}_3$  were also checked for the regeneration of the used optode by immersion of the used optode to the acids solution (0.01, 0.05, and  $0.10 \text{ mol L}^{-1}$ ) for 180 s. The results showed that the optodes could be regenerated in  $0.10 \text{ mol L}^{-1}$   $\text{HNO}_3$  solution. Therefore, each optode can be used several times for  $\text{Hg}^{2+}$  analysis.

### Selectivity

The selectivity behavior which is the relative optode response for the primary ion over other ions present in solution, is one of the most important characteristics of any ion-selective optical sensor. To investigate the selectivity of the proposed membrane sensor, the fluorescence intensity of a fixed concentration of  $\text{Hg}^{2+}$  ( $1.0 \times 10^{-10} \text{ mol L}^{-1}$ ) in a solution of pH 6.0 was measured before ( $F_0$ ) and after addition ( $F$ ) of some potentially interfering ions such as  $\text{K}^+$ ,  $\text{Na}^+$ ,  $\text{Mg}^{2+}$ ,  $\text{Ca}^{2+}$ ,  $\text{Ba}^{2+}$ ,  $\text{Sr}^{2+}$ ,  $\text{Al}^{3+}$ ,  $\text{Co}^{2+}$ ,  $\text{Ni}^{2+}$ ,  $\text{Cu}^{2+}$ ,  $\text{Zn}^{2+}$ ,  $\text{Pb}^{2+}$ ,  $\text{Ag}^+$ ,  $\text{Cd}^{2+}$ ,  $\text{Mn}^{2+}$ ,  $\text{Fe}^{3+}$  and  $\text{Cr}^{3+}$  at concentrations up to  $1.0 \times 10^{-2} \text{ mol L}^{-1}$ . The resulting relative error is defined as  $\text{RE} (\%) = [(F - F_0)/F_0] \times 100$ . The experimental results (Fig. 12) revealed that most alkali, alkaline earth, and many transition metal cations don't show significant interference on the  $\text{Hg}^{2+}$  assay, where the observed relative error was less than  $\pm 5\%$  relative error, which is considered as tolerable.

### Analytical Applications

To assess the applicability of the proposed chemosensor to real samples, we further conducted  $\text{Hg}^{2+}$  detection in different

human hair samples, urine samples, collected from dentists and well water samples. The water samples were collected from three different places in Tabuk (Saudi Arabia). For evaluating the accuracy of the method, a comparison between results obtained by proposed method and cold vapor atomic absorption spectrometry (CVAAS) was performed. As can be seen in Table 3, the results obtained for both methods have good agreements.

**Table 3** Determination of  $\text{Hg}^{2+}$  in real samples of six replicate measurements

Sample	Amount of mercury <sup>a</sup>		Relative error (%)
	CVAAS	Proposed sensor	
Hair samples <sup>c</sup>			
1	172.90 <sup>a</sup> ±0.90 <sup>b</sup>	173.64 <sup>a</sup> ±0.80 <sup>b</sup>	−0.43
2	279.50 <sup>a</sup> ±4.40 <sup>b</sup>	277.43±1.40 <sup>b</sup>	0.74
3	197.50 <sup>a</sup> ±2.40 <sup>b</sup>	1.96.43±1.25 <sup>b</sup>	0.56
Urine samples <sup>d</sup>			
1	3.47 <sup>a</sup> ±0.05 <sup>b</sup>	3.45 <sup>a</sup> ±0.05 <sup>b</sup>	0.58
2	3.80 <sup>a</sup> ±0.08 <sup>b</sup>	3.83 <sup>a</sup> ±0.08 <sup>b</sup>	−0.78
3	3.65 <sup>a</sup> ±0.02 <sup>b</sup>	3.62 <sup>a</sup> ±0.02 <sup>b</sup>	0.82
Well water samples <sup>d</sup>			
1	1.72 <sup>a</sup> ±0.03 <sup>b</sup>	1.71 <sup>a</sup> ±0.02 <sup>b</sup>	0.58
2	1.10 <sup>a</sup> ±0.07 <sup>b</sup>	1.12 <sup>a</sup> ±0.06 <sup>b</sup>	−1.82
3	1.45 <sup>a</sup> ±0.05 <sup>b</sup>	1.43 <sup>a</sup> ±0.07 <sup>b</sup>	1.38

<sup>a</sup> Mean values of three determinations

<sup>b</sup> Standard deviation

<sup>c</sup> Reported value:  $\mu\text{gKg}^{-1}$

<sup>d</sup> Reported value:  $\mu\text{gL}^{-1}$

**Table 4** Comparison between the proposed optode for determination of  $\text{Hg}^{2+}$  and recent literatures

Reagent	Membrane	Working range (mol L <sup>-1</sup> )	Limit of detection (mol L <sup>-1</sup> )	Response time (Sec.)	Signal	Reference
2-(5-amino-3,4-dicyano-2H-pyrrol-2-ylidene)-1,1,2-tricyanoethanide	Sol-gel thin film of (PVF/SiO <sub>2</sub> ),	$5.0 \times 10^{-3} - 5.0 \times 10^{-4}$	$5.0 \times 10^{-5}$	600	Absorbance	[91]
1-(2-Pyridylazo)-2-naphthol (PAN)	PVC	$1.0 \times 10^{-5} - 1.0 \times 10^{-3}$	$5.5 \times 10^{-7}$	NR <sup>a</sup>	Absorbance	[92]
Dithizone	Triacetylcellulose	$7.5 \times 10^{-7} - 9.7 \times 10^{-6}$	$1.0 \times 10^{-7}$	180–540	Absorbance	[93]
1-(dansylamidopropyl)-1-aza-4,10-dithia-7-oxacyclododecane	PVC	$1.0 \times 10^{-4} - 5.0 \times 10^{-12}$	$8.0 \times 10^{-13}$	60	Fluorescence	[82]
Trityl-picolinamide (T-Pico)	PVC	$5.0 \times 10^{-7} - 5.0 \times 10^{-4}$	$5.0 \times 10^{-7}$	300–600	Absorbance	[94]
4-(2-Pyridylazo)-resorcinol	Triacetylcellulose	$5.0 \times 10^{-6} - 3.4 \times 10^{-3}$	$1.5 \times 10^{-6}$	1200	Fluorescence	[95]
4-hydroxy salophen	Triacetylcellulose	$1.0 \times 10^{-6} - 1.0 \times 10^{-2}$	$1.3 \times 10^{-7}$	300–360	Absorbance	[96]
2-mercaptopyrimidine (2-MP)	PVC	$2.0 \times 10^{-9} - 2.0 \times 10^{-5}$	$4.0 \times 10^{-10}$	≤45 s	Absorbance	[73]
2-mercapto-2-thiazoline (MTZ)	PVC	$2.0 \times 10^{-10} - 1.5 \times 10^{-5}$	$5.0 \times 10^{-11}$ M	150 s	Absorbance	[97]
4-(2-Pyridylazo)resorcinol (PAR)	Tri-(2-ethylhexyl) phosphate plasticized cellulose triacetate	$\times 10^{-6} - 6.6 \times 10^{-6}$	$1.1 \times 10^{-6}$	300	Absorbance	[98]
1,3-Di(2-methoxyphenyl)triazene	PVC	$2.1 \times 10^{-7} - 1.2 \times 10^{-4}$	$2.0 \times 10^{-7}$	300	Absorbance	[99]
4-phenyl-2,6-bis(2,3,5,6-tetrahydrobenzo[b][1,4,7]trioxonon-9-yl)pyrylium perchlorate	PVC	$2.95 \times 10^{-10} - 3.20 \times 10^{-3}$	$1.01 \times 10^{-10}$	120	Absorbance	[100]
Tetra(p-dimethylaminophenyl) porphyrin	PVC	$4.0 \times 10^{-8} - 4.0 \times 10^{-6}$	$8.0 \times 10^{-9}$	300	Fluorescence	[101]
4-phenyl-2,6-bis(2,3,5,6-tetrahydrobenzo[b][1,4,7]trioxonon-9-yl)pyrylium perchlorate	So-gel	$1.52 \times 10^{-9} - 1.70 \times 10^{-2}$	$1.11 \times 10^{-9}$	180	Absorbance	[102]
4-Ethyl-5-hydroxy-5,6-di-pyridin-2-yl-4,5-dihydro-2H-[1, 2, 4]triazine-3-thione	PVC	$5.0 \times 10^{-10} - 5.0 \times 10^{-5}$	$1.8 \times 10^{-10}$	360	Fluorescence	[63]
Hexathiacyclooctadecane						
2-[(2-sulfanyphenyl)ethanimidoyl]phenol	Sol-gel	$1.0 \times 10^{-2} - 1.0 \times 10^{-5}$	$1.0 \times 10^{-6}$	180	Absorbance	[68]
(1Z,2Z)-N_1,N_2-dihydroxy-N1,N2-dipyridin-2-ylethanediimide	PVC	$5.78 \times 10^{-9} - 1.05 \times 10^{-3}$	$1.71 \times 10^{-9}$	< 120	Fluorescence	[103]
Tetraphenyl-12-crown-4	PVC	$1.0 \times 10^{-9} - 9.5 \times 10^{-5}$	$8.1 \times 10^{-10}$	100 s	Absorbance	[45]
Indigo carmine; N-cetyl pyridinium chloride (IC-N-CPC)	Triacetylcellulose	$2.4 \times 10^{-5} - 4.7 \times 10^{-4}$	$7.2 \times 10^{-6}$	480–600	Absorbance	[104]
Rhodamine B derivative (RND)	PVC	$1.0 \times 10^{-9} - 2.0 \times 10^{-3}$ M	$8.1 \times 10^{-10}$	180–900	Fluorescence.	[105]
1,15-diaza-3,4,12,13-dibenzo-8-oxa-16,18-pyridin-5,11-dithiacyclo octadecane-2,14-dione	PVC	$1.0 \times 10^{-12} - 8.6 \times 10^{-4}$	$5.3 \times 10^{-13}$	49.8	Absorbance	[54]
N,N'-bis(2-aminothiophenol)benzene-1,2-dicarboxaldehyde (ATBD)	PVC	$1.0 \times 10^{-10} - 8.6 \times 10^{-2}$	$7.23 \times 10^{-11}$	< 35		Current method

<sup>a</sup> NR not reported

## Comparison of the Proposed Optode with Previously Reported Methods

The present proposed sensor was compared to recently  $\text{Hg}^{2+}$  sensing methods based on S-containing, Schiff bases or immobilized ionophore (Table 4) [45, 54, 63, 68, 73, 82, 91–105]. Each of the reported method has its own merits, but each method also offers some problems such as poor reproducibility, limited sample adaptability, high cost, well-controlled experimental conditions, complicated sample-pretreatment, some inherent interference and time consuming procedures. As can be seen, the proposed sensor shows better selectivity, better LOD ( $7.23 \times 10^{-11} \text{ mol L}^{-1}$ ) and short response time (35 s) relative to other reported methods.

## Conclusion

In conclusion, an efficient, easy, low-cost and high selective fluoroionophore is developed and potentially utilized for selective and sensitive determination of  $\text{Hg}^{2+}$  based on a novel dithiol Schiff base namely: N,N'-bis(2-aminothiophenol)benzene-1,2-dicarboxaldehyde (ATBD) immobilized within a plasticized PVC membrane, with good optical and mechanical properties. The sensor showed short response time (35 s), appropriate linear dynamic range ( $1.0 \times 10^{-10} - 1.0 \times 10^{-2} \text{ mol L}^{-1}$ ) and low detection limit ( $7.23 \times 10^{-11} \text{ mol L}^{-1}$ ). The proposed fluorescence optode was successfully applied to the determination of  $\text{Hg}^{2+}$  ions in hair, urine and well water samples.

## References

- de Silva AP, Gunaratne HQN, Gunnlaugsson T, Huxley AJM, McCoy CP, Rademacher JT, Rice TE (1997) ChemInform abstract: signaling recognition events with fluorescent sensors and switches. *Chem Rev* 97(5):1515–1566
- Valeur B, Leray I (2000) Design principles of fluorescent molecular sensors for cation recognition. *Coord Chem Rev* 205(1):3–40
- Oehme I, Wolfbeis OS (1997) Optical sensors for determination of heavy metal ions. *Microchim Acta* 126(3–4):177–192
- Hisamoto H, Suzuki K (1999) Ion-selective optodes: current developments and future prospects. *Trac-Trend Anal Chem* 18(8):513–524
- Oehme I, Praltes S, Wolfbeis OS, Mohr GJ (1998) The effect of polymeric supports and methods of immobilization on the performance of an optical copper(II)-sensitive membrane based on the colourimetric reagent Zincon. *Talanta* 47(3):595–604
- Zevin M, Reisfeld R, Oehme I, Wolfbeis OS (1997) Sol-gel derived optical coatings for determination of chromate. *Sens Actuat B* 39(1–3):235–238
- Cabello-Carramolino G, Petit-Dominguez M (2008) Application of new sol-gel electrochemical sensors to the determination of trace mercury. *Anal Chim Acta* 614(1):103–111
- Bakker E, Buhlmann P, Pretsch E (1997) Carrier-based ion-selective electrodes and bulk optodes. 1. General characteristics. *Chem Rev* 97(8):3083–3132
- Bühlmann P, Pretsch E, Bakker E (1998) Carrier based ion-selective electrodes and bulk optodes. 2. Ionophores for potentiometric and optical sensors. *Chem Rev* 98(4):1593–1687
- Brook TE, Narayanaswamy R (1998) Polymeric films in optical gas sensors. *Sens Actuat B* 51(1–3):77–83
- Boening DW (2000) Ecological effects, transport, and fate of mercury: a general review. *Chemosphere* 40(12):1335–1351
- Ha-Thi M, Penhoat M, Mochelet V, Leray I (2007) Highly selective and sensitive phosphane sulfide derivative for the detection of  $\text{Hg}^{2+}$  in an organo-aqueous medium. *Org Lett* 9(6):1133–1136
- Wang Q, Kim D, Dionysiou DD, Sorial GA, Timberlake D (2004) Sources and remediation for mercury contamination in aquatic systems—a literature review. *Environ Pollut* 131(2):323–336
- Drinking water standards and health advisories, EPA 822-R-04-005, U.S. Environmental Protection Agency, Washington, DC, 2004 (U.S. Environmental Protection Agency Site at <http://www.epa.gov/safewater/dwh/c-ioc/nickel.html>) and WHO's Drinking Water Standards 2006 ([http://www.who.int/water\\_sanitation\\_health/dwq/gdwq0506.pdf](http://www.who.int/water_sanitation_health/dwq/gdwq0506.pdf))
- Anselmi A, Tittarelli P, Katskov DA (2002) Determination of trace elements in automotive fuels by filter furnace atomic absorption spectrometry. *Spectrochim Acta B* 57(3):403–411
- Baralkiewicz D, Gramowska H, Kózka M, Kanecka A (2005) Determination of mercury in sewage sludge by direct slurry sampling graphite furnace atomic absorption spectrometry. *Spectrochim Acta B* 60(3):409–413
- Madden JT, Fitzgerald N (2009) Investigation of ultraviolet photolysis vapor generation with in-atomizer trapping graphite furnace atomic absorption spectrometry for the determination of mercury. *Spectrochim Acta B* 64(9):925–927
- Araujo RGO, Rennan GO, Vignola F, Castilho INB, Borges DLG, Welz B, Vale MGR, Smichowski P, Ferreira SLC, Becker-Ross H (2011) Determination of mercury in airborne particulate matter collected on glass fiber filters using high-resolution continuum source graphite furnace atomic absorption spectrometry and direct solid sampling. *Spectrochim Acta B* 66(5):378–382
- Harrington CF, Merson SA, D' Silva TMD (2004) Method to reduce the memory effect of mercury in the analysis of fish tissue using inductively coupled plasma mass spectrometry. *Anal Chim Acta* 505(2):247–254
- Anthemidis AN, Zachariadis GA, Michos CE, Stratis JA (2004) Time-based on-line preconcentration cold vapour generation procedure for ultra-trace mercury determination with inductively coupled plasma atomic emission spectrometry. *Anal Bioanal Chem* 379(5–6):764–769
- Krata A, Bulska E (2005) Critical evaluation of analytical performance of atomic absorption spectrometry and inductively coupled plasma mass spectrometry for mercury determination. *Spectrochim Acta B* 60(3):345–350
- Martinez T, Lartigue J, Zarazua G, Avila-Perez P, Navarrete M, Tejeda S (2008) Application of the Total Reflection X-ray Fluorescence technique to trace elements determination in tobacco. *Spectrochim Acta B* 63(12):1469–1472
- Bennun L, Gomez J (1997) Determination of mercury by total-reflection X-ray fluorescence using amalgamation with gold. *Spectrochim Acta B* 52(8):1195–1200
- Osawa T, Hatsukawa Y, Appel PWU, Matsue H (2011) Mercury and gold concentrations of highly polluted environmental samples determined using prompt gamma-ray analysis and instrument neutron activation analysis. *Nucl Instrum Meth B* 269(8):17–720
- Sysalová J, Kučera J, Fikrle M, Drtinová B (2013) Determination of the total mercury in contaminated soils by direct solid sampling atomic absorption spectrometry using an AMA-254 device and



- radiochemical neutron activation analysis. *Microchem J* 110:691–694
26. Romero V, Costas-Mora I, Lavilla I, Bendicho C (2011) Cold vapor-solid phase microextraction using amalgamation in different Pd-based substrates combined with direct thermal desorption in a modified absorption cell for the determination of Hg by atomic absorption spectrometry. *Spectrochim Acta B* 66(2):156–162
  27. Gil S, Lavilla I, Bendicho C (2007) Green method for ultrasensitive determination of Hg in natural waters by electrothermal-atomic absorption spectrometry following sono-induced cold vapor generation and 'in-atomizer trapping. *Spectrochim Acta B* 62(1):69–75
  28. Sardans J, Montes F, Peñuelas J (2010) Determination of As, Cd, Cu, Hg and Pb in biological samples by modern electrothermal atomic absorption spectrometry. *Spectrochim Acta B* 65(2):97–112
  29. Jiang X, Gan W, Wan L, Zhang H, He Y (2010) Determination of mercury by electrochemical cold vapor generation atomic fluorescence spectrometry using polyaniline modified graphite electrode as cathode. *Spectrochim Acta B* 65(2):171–175
  30. Shahar T, Tal N, Mandler D (2013) The synthesis and characterization of thiol-based aryl diazonium modified glassy carbon electrode for the voltammetric determination of low levels of Hg(II). *J Solid State Electrochem* 17(6):1543–1552
  31. Filho NLD, do Carmo DR, Rosa AH (2006) An electroanalytical application of 2-aminothiazole-modified silica gel after adsorption and separation of Hg(II) from heavy metals in aqueous solution. *Electrochim Acta* 52(3):965–972
  32. do Nascimento FH, Masini JC (2012) Complexation of Hg(II) by humic acid studied by square wave stripping voltammetry at screen-printed gold electrodes. *Talanta* 100:57–63
  33. Chaiyo S, Chailapakul O, Sakai T, Teshima N, Siangproh W (2013) Highly sensitive determination of trace copper in food by adsorptive stripping voltammetry in the presence of 1,10-phenanthroline. *Talanta* 108:1–6
  34. Harrington CF (2000) The speciation of mercury and organomercury compounds by using high-performance liquid chromatography. *TrAC* 19(2–3):167–179
  35. Bramanti E, Lomonte C, Onor M, Zamboni R, D'Ulivo A, Raspi G (2005) Mercury speciation by liquid chromatography coupled with on-line chemical vapour generation and atomic fluorescence spectrometric detection (LC–CVGAFS). *Talanta* 66(3):762–768
  36. Wang M, Feng WY, Shi JW, Zhang F, Wang B, Zhu MT, Li B, Zhao YL, Chai ZF (2007) Development of a mild mercaptoethanol extraction method for determination of mercury species in biological samples by HPLC–ICP-MS. *Talanta* 71(5):2034–2039
  37. Liu Q (2010) Direct determination of mercury in white vinegar by matrix assisted photochemical vapor generation atomic fluorescence spectrometry detection. *Spectrochim Acta B* 65(7):587–590
  38. Fakhari AR, Ganjali MR, Shamsipur M (1997) PVC-based hexathia-18-crown-6-tetraone sensor for mercury(II) ions. *Anal Chem* 69(18):3693–3696
  39. Perez-Marin L, Lopez-Valdivia H, Avila-Perez P, Chamero JA, Lopez-Valdivia H (2000) Mercury(II) ion-selective electrode. Study of 1,3- diphenylthiourea as ionophore. *Analyst* 125(10):1787–1790
  40. Ugo P, Mortto L, Bertoneell P, Wang J (1998) Determination of trace mercury in saltwaters at screen-printed electrodes modified with sumichelate Q10R. *Electroanal* 10(15):1017–1021
  41. Mandal AK, Suresh M, Suresh E, Mishra SK, Mishra S, Das A (2010) A chemosensor for heavytransition metal ions in mixed aqueous-organic media. *Sens Actuat B* 145(1):32–38
  42. Zou Q, Tian H (2010) Chemodosimeters for mercury(II) and methylmercury(I) based on 2,1,3-benzothiadiazole. *Sens Actuat B* 149(1):20–27
  43. Zou Q, Jin J, Xu B, Ding L, Tian H (2011) New photochromic chemosensors for Hg<sup>2+</sup> and F<sup>-</sup>. *Tetrahedron* 67(5):915–921
  44. Ebdelli R, Rouis A, Mlika R, Bonnamour I, Jaffrezic N, Ouada J, Davenas HB (2012) Ion sensing film optodes based on chromogenic calix[4]arene: application to the detection of Hg<sup>2+</sup>, Ni<sup>2+</sup> and Eu<sup>3+</sup> ions. *J Incl Phenom Macrocycl Chem* 73(1–4):109–117
  45. Firooza AR, Movahedia M, Ensafi AA (2012) Selective and sensitive optical chemical sensor for the determination of Hg(II) ions based on tetrathia-12-crown-4 and chromoionophore I. *Sens Actuat B* 171–172:492–498
  46. Martínez R, Espinosa A, Tárraga A, Molina P (2010) A new bis(pyrenyl)azadiene-based probe for the colorimetric and fluorescent sensing of Cu(II) and Hg(II). *Tetrahedron* 66(21):3662–3667
  47. Kaura P, Kaura S, Kasettic Y, Bharatam PV, Singh K (2010) A new colorimetric chemodosimeter for Hg<sup>2+</sup> based on charge transfer compound of Nmethylpyrrole with TCNQ. *Talanta* 83(2):644–650
  48. Bao WT, Jian LJ, Bing BC, Qi L, Hong Y, Qiang XY, Ming ZY (2013) A highly selective colorimetric sensor for Hg<sup>2+</sup> based on a copper (II) complex of thiosemicarbazone in aqueous solutions. *Sci China Chem* 56(7):923–927
  49. Hamzeh AY, Abdoli A (2010) Sol–gel derived highly selective optical sensor for sensitive determination of the mercury(II) ion in solution. *J Hazard Mater* 178(1–3):713–717
  50. Al-Kady AS, Abdelmonem FI (2013) Highly sensitive and selective spectrophotometric detection of trace amounts of Hg<sup>2+</sup> in environmental and biological samples based on 2,4,7-triamino-6-phenylpteridine. *Sens Actuat B* 182:87–94
  51. Lu F, Yamamura M, Nabeshima T (2013) A highly selective and sensitive ratiometric chemodosimeter for Hg<sup>2+</sup> ions based on an iridium(III) complex via thioacetal deprotection reaction. *Dalton Trans* 42(34):12093–12100
  52. Udhayakumari D, Velmathi S (2013) Colorimetric and fluorescent sensor for selective sensing of Hg<sup>2+</sup> ions in semi aqueous medium. *J Lumin* 136:117–121
  53. Dong Z, Tian X, Chen Y, Hou J, Guo Y, Sun J, Ma J (2013) A highly selective fluorescent chemosensor for Hg<sup>2+</sup> based on rhodamine B and its application as a molecular logic gate. *Dyes Pigments* 97(2):324–329
  54. Firooz AR, Ensafi AA, Hajyani Z (2013) A highly sensitive and selective bulk optode based on dithiacyclooctadecane derivative incorporating chromoionophore V for determination of ultra trace amount of Hg(II). *Sens Actuat B* 177:710–716
  55. Mandal S, Banerjee A, Lohar S, Chattopadhyay A, Sarkar B, Mukhopadhyay SK, Sahana A, Das D (2013) Selective sensing of Hg<sup>2+</sup> using rhodamine–thiophene conjugate: red light emission and visual detection of intracellular Hg<sup>2+</sup> at nanomolar level. *J Hazard Mater* 261:198–205
  56. Zhang N, Li G, Cheng Z, Zuo X (2012) Rhodamine B immobilized on hollow Au–HMS material for naked-eye detection of Hg<sup>2+</sup> in aqueous media. *J Hazard Mater* 229–230:404–410
  57. Vasimalai N, Sheeba G, John SA (2012) Ultrasensitive fluorescence-quenched chemosensor for Hg(II) in aqueous solution based on mercaptothiadiazole capped silver nanoparticles. *J Hazard Mater* 213–214:193–199
  58. Wang F, Nam S, Guo Z, Park S, Yoon J (2012) A new rhodamine derivative bearing benzothiazole and thiocarbonyl moieties as a highly selective fluorescent and colorimetric chemodosimeter for Hg<sup>2+</sup>. *Sens Actuat B* 161(1):948–953
  59. García-Beltrán O, Mena N, Berrios TA, Castro EA, Cassels BK, Núñez MT, Aliaga ME (2012) A selective fluorescent probe for the detection of mercury (II) in aqueous media and its applications in living cells. *Tetrahedron Lett* 53(48):6598–6601
  60. Thamaraj V, Pitchumani K (2012) An acyclic, dansyl based colorimetric and fluorescent chemosensor for Hg(II) via twisted intramolecular charge transfer (TICT). *Anal Chim Acta* 751:171–175
  61. Wang F, Nam S, Guo Z, Park S, Yoon J (2012) A new rhodamine derivative bearing benzothiazole and thiocarbonyl moieties as a



- highly selective fluorescent and colorimetric chemodosimeter for  $\text{Hg}^{2+}$ . *Sens. Actuators B* 161:948–953
62. Liu W, Chen J, Xu L, Wu J, Xu H, Zhang H, Wang P (2012) Reversible “off-on” fluorescent chemosensor for  $\text{Hg}^{2+}$  based on rhodamine derivative. *Spectrochim Acta A* 85(1):38–42
  63. Aksuner N, Basaran B, Henden E, Yilmaz I, Cukurovali A (2011) A sensitive and selective fluorescent sensor for the determination of mercury(II) based on a novel triazine-thione derivative. *Dyes Pigments* 88(2):143–148
  64. Li J, Meng J, Huang X, Cheng Y, Zhu C (2010) Highly selective fluorescent sensor for  $\text{Hg}^{2+}$  based on the water-soluble poly(p-phenyleneethynylene). *Polymer* 51:3425–3430
  65. Kim HJ, Park JE, Choi MG, Ahn S, Chang S (2010) Selective chromogenic and fluorogenic signalling of  $\text{Hg}^{2+}$  ions using a fluorescein-coumarin conjugate. *Dyes Pigments* 84(1):54–58
  66. Wang J, Huang L, Xue M, Liu L, Wang Y, Gao L, Zhu J, Zou Z (2008) Developing a novel fluorescence chemosensor by self-assembly of Bis-Schiff base within the channel of mesoporous SBA-15 for sensitive detecting of  $\text{Hg}^{2+}$  ions. *Appl Surf Sci* 254(17):5329–5335
  67. Bozkurt SS, Cavas L (2009) Can  $\text{Hg(II)}$  be determined via quenching of the emission of green fluorescent protein from anemone sulcata var. smaragdina. *Appl Biochem Biotechnol* 158(1):51–58
  68. Alizadeh K, Parooi R, Hashemi P, Rezaei B, Ganjali MR (2011) A new Schiff's base ligand immobilized agarose membrane optical sensor for selective monitoring of mercury ion. *J Hazard Mater* 186(2–3):1794–1800
  69. Ganjali MR, Poursaberi T, Hajiagha-Babaei L, Rouhani S, Yousefi M, Kargar-Razi M, Moghimi A, Aghabozorg H, Shamsipur M (2001) Highly selective and sensitive copper(II) membrane coated graphite electrode based on a recently synthesized Schiff's base. *Anal Chim Acta* 440(2):81–87
  70. Gholivand MB, Ahmadi F, Rafiee E (2006) A novel Al(III)-selective electrochemical sensor based on N, N-bis(salicylidene)-1,2-phenylenediamine complexes. *Electroanal* 18(16):1620–1626
  71. Ganjali MR, Rezapour M, Norouzi P, Salavati-Niasari M (2005) A new pentadentate S-N Schiff's-base as a novel ionophore in construction of a novel Gd(III) membrane sensor. *Electroanal* 1:2032–2036
  72. Schwarzenbach G, Flaselika H, Irving H (1969) *Complexometric titrations*, 2nd edn. Methuen, London
  73. Khezri B, Amini MK, Firooz AR (2008) An optical chemical sensor for mercury ion based on 2-mercaptopyrimidine in PVC membrane. *Anal Bioanal Chem* 390(7):1943–1950
  74. Amini MK, Momeni-Isfahani T, Khorasani JH, Pourhossein M (2004) Development of an optical chemical sensor based on 2-(5-bromo-2-pyridylazo)-5-(diethylamino)phenol in Nafion for determination of nickel ion. *Talanta* 63(3):713–720
  75. Pournaghi-Azar MH, Dastangoo H (2000) Differential pulse anodic stripping voltammetry of copper in dichloromethane: application to the analysis of human hair. *Anal Chim Acta* 405(1–2):135–144
  76. Suzuki T, Akagi H, Arimura K, Ando T, Sakamoto M, Satoh H, Naganuma A, Futatsuka M, Matsuyama A (2004) *Mercury analysis manual*. Ministry of the Environment, Japan
  77. Mantyla DG, Wright OD (1976) Mercury toxicity in the dental office: a neglected problem. *JADA* 92(6):1189–1194
  78. Lakowicz JR (1999) *Principles of fluorescence spectroscopy*, 2nd edn. Kluwer Academic/Plenum Publishers, New York
  79. Morales-Bahnik A, Czolk R, Reichert J, Ache HJ (1993) An optochemical sensor for Cd(II) and Hg(II) based on a porphyrin immobilized on Nafion® membranes. *Sens Actuators B* 13(1–3):424–426
  80. Rosatzin T, Bakker E, Suzuki K, Simon W (1993) Lipophilic and immobilized anionic additives in solvent polymeric membranes of cation-selective chemical sensors. *Anal Chim Acta* 280(2):197–208
  81. Abdel Aziz AA (2013) A novel highly sensitive and selective optical sensor based on a symmetric tetradentate Schiff-base embedded in PVC polymeric film for determination of  $\text{Zn}^{2+}$  ion in real samples. *J Lumin* 143:663–669
  82. Shamsipur M, Hosseini M, Alizadeh K, Alizadeh N, Yari A, Caltagirone C, Lippolis V (2005) Novel fluorimetric bulk optode membrane based on a dansylamidopropyl pendant arm derivative of 1aza4,10dithia7oxacyclododecane ([12]aneNS2O) for selective subnanomolar detection of Hg(II) ions. *Anal Chim Acta* 533(1):17–24
  83. Blake AJ, Schröder M (1990) Chemistry of thioether macrocyclic complexes. *Adv Inorg Chem* 35:1–80
  84. Housecroft CE (1992) Silver. *Coord Chem Rev* 115:141–161
  85. Yilmaz I, Temel H, Alp H (2008) Synthesis, electrochemistry and in situ spectroelectrochemistry of a new Co(III) thio Schiff-base complex with N, N-bis(2-aminothiophenol)-1,4-bis(carboxylidene phenoxy)butane. *Polyhedron* 27(1):125–132
  86. Vicente M, Bastida R, Lodeiro C, Macias A, Parola AJ, Valencia L, Spey SE (2003) Metal complexes with a new  $\text{N}_4\text{O}_3$  amine pendant-armed macrocyclic ligand: synthesis, characterization, crystal structures, and fluorescence studies. *Inorg Chem* 42(21):6768–6779
  87. Zengin H, Dolaz M, Golcu A (2009) Preparation, photoluminescence and antimicrobial activity of loracarbef and its various complexes. *Curr Anal Chem* 5(4):358–362
  88. Cai LZ, Chen WT, Wang MS, Guo GC, Huang JS (2004) Syntheses, structures and luminescent properties of four new 1D lanthanide complexes with 2-thiopheneacetic acid ligand. *Inorg Chem Commun* 7(5):611–614
  89. Chan WH, Yang RH, Mo T, Wang KM (2002) Lead-selective fluorescent optode membrane based on 3,3',5,5'-tetramethyl-N-(9-anthrylmethyl)benzidine. *Anal Chim Acta* 460(1):123–132
  90. Cao YD, Zheng QY, Chen CF, Huang ZT (2003) A new fluorescent chemosensor for transition metal cations and on/off molecular switch controlled by pH. *Tetrahedron Lett* 44(25):4751–4755
  91. Flamini A, Panusa A (1997) Development of optochemical sensors for Hg(II), based on immobilized 2-(5-amino-3,4-dicyano-2H-pyrrol-2-ylidene)-1,1,2-tricyanoethanide. *Sens Actuators B* 42(1):39–46
  92. Sanchez-Pedreno C, Ortuno JA, Albero MI, Garcia MS, Valero MV (2000) Development of a new bulk optode membrane for the determination of mercury(II). *Anal Chim Acta* 414(1–2):195–203
  93. Safavi A, Bagheri M (2004) Design and characteristics of a mercury (II) optode based on immobilization of dithizone on a triacetylcellulose membrane. *Sens Actuators B* 99(2–3):608–612
  94. Nuriman BK, Dam HH, Reinhoudt DN, Verboom W (2007) Development of a disposable mercury ion-selective optode based on trityl-picolinamide as ionophore. *Anal Chim Acta* 591(2):208–213
  95. Ensafi AA, Fooladgar M (2006) Development of a mercury optical sensor based on immobilization of 4-(2-pyridylazo)-resorcinol on a triacetylcellulose membrane. *Sens Actuators B* 113(1):88–93
  96. Ensafi AA, Far AK, Meghdadi S (2008) Highly selective optical sensor for mercury assay based on covalent immobilization of 4-hydroxy salophen on a triacetylcellulose membrane. *Sens Actuators B* 133(1):84–90
  97. Amini MK, Khezri B, Firooz AR (2008) Development of a highly sensitive and selective optical chemical sensor for batch and flow-through determination of mercury ion. *Sens Actuators B* 131(2):470–478
  98. Kalyan Y, Pandey AK, Bhagat PR, Acharya R, Natarajan V, Naidu GRK, Reddy AVR (2009) Membrane optode for mercury(II) determination in aqueous samples. *J Hazard Mater* 166(1):377–382
  99. Ensafi AA, Fooladgar M (2009) A sensitive and selective bulk optode for determination of Hg(II) based on hexathiacyclooctadecane and chromoionophore V. *Sens Actuators B* 136(2):326–331

100. Yari A, Papi F (2009) A of mercury (II) by development and characterization of a PVC-based optical sensor. *Sens Actuat B* 138(2):467–473
101. Yang Y, Jiang J, Shen G, Yu R (2009) An optical sensor for mercury ion based on the fluorescence quenching of tetra(p-dimethylaminophenyl)porphyrin. *Anal Chim Acta* 636(2–3):83–88
102. Yari A, Abdoli HA (2010) Sol–gel derived highly selective optical sensor for sensitive determination of the mercury(II) ion in solution. *J Hazard Mater* 178(1–3):713–717
103. Yari A, Papi F (2011) Ultra trace mercury(II) detection by a highly selective new optical sensor. *Sens Actuat B* 160(1):698–704
104. Tavallali H, Shaabanpur E, Vahdati P (2012) A highly selective optode for determination of Hg (II) by a modified immobilization of indigo carmine on a triacetylcellulose membrane. *Spectrochim Acta A* 89:216–221
105. Ling L, Zhao Y, Du J, Xiao D (2012) An optical sensor for mercuric ion based on immobilization of Rhodamine B derivative in PVC membrane. *Talanta* 91:65–71